Microchimica Acta (2022) 189: 181
https://doi.org/10.1007/s00604-022-05287-5

ORIGINAL PAPER

A catalyst-free co-reaction system of long-lasting and intensive chemiluminescence applied to the detection of alkaline phosphatase

Xin Jie Wu[1] · Chang Ping Yang[1] · Zhong Wei Jiang[1] · Si Yu Xiao[1] · Xiao Yan Wang[1] · Cong Yi Hu[1] · Shu Jun Zhen[1] · Dong Mei Wang[1] · Cheng Zhi Huang[2] · Yuan Fang Li[1]

Received: 16 December 2021 / Accepted: 17 March 2022 / Published online: 8 April 2022

Abstract

A catalyst-free co-reaction luminol-H_2O_2–$K_2S_2O_8$ chemiluminescence (CL) system was developed, with long-life and high-intensity emission, and CL emission lasting for 6 h. A possible mechanism of persistent and intense emission in this CL system was discussed in the context of CL spectra, cyclic voltammetry, electron spin resonance (ESR), and the effects of radical scavengers on luminol-H_2O_2–$K_2S_2O_8$ system. H_2O_2 and $K_2S_2O_8$ co-reactants can promote each other to continuously generate corresponding radicals ($OH^{\bullet}$, $^1O_2$, $O_2^{\bullet-}$, $SO_4^{\bullet-}$) that trigger the CL emission of luminol. H_2O_2 can also be constantly produced by the reaction of $K_2S_2O_8$ and H_2O to further extend the persistence of this CL system. CL emission can be quenched via ascorbic acid (AA), which can be generated through hydrolysis reaction of L-ascorbic acid 2-phosphate trisodium salt (AAP) and alkaline phosphatase (ALP). Next, a CL-based method was established for the detection of ALP with good linearity from 0.08 to 5 $U{\cdot}L^{-1}$ and a limit of detection of 0.049 $U{\cdot}L^{-1}$. The proposed method was used to detect ALP in human serum samples.

Keywords Chemiluminescence · Luminol · Co-reactants · Alkaline phosphatase

Introduction

Due to the low detection limit, high-throughput detection, and fast analysis, chemiluminescence (CL) has been considered a prospective analytical method [1]. However, most CL reactions are flash-type and quenched quickly, which usually results to measurement errors that greatly impede their applications [2]. In contrast, the glow-type CL has long-lasting emission that improves analytical accuracy and reproducibility. Hence, developing high-intensity glow-type CL systems is an active research topic of CL.

Some enzymes involved CL reactions and the peroxyoxalate ester CL reagents are often used in CL sensing due to long-lasting emission [3]. For enzyme-involved CL reactions, the mechanism of long-life CL emission is likely the excessive substrates and conversion of enzymes [4]. However, this kind of CL system requires stricter conditions in order to avoid enzyme inactivation [5]. Among CL systems with peroxyoxalate esters, the mechanism of long-lasting CL emission is the successive supply of excess oxalate and fluorophore. These continuously generate activated intermediate complexes [6]. However, the poor solubility of peroxyoxalate esters in water greatly hinders the prospect of this kind of CL system in biosensing [7].

In 2017, Cui et al. made great progress in the development of long-lasting CL systems and proposed a slow-diffusion-controlled CL mechanism [8]. Based on this mechanism, Ding et al. proposed a new long-life CL system, which was composed of Dox-ABEI chimeric magnetic DNA hydrogel (MDH) [9]. The Liu group employed MOF-Pt as a catalyst to improve long-lasting CL of ABEI/Co^{2+}/CS hydrogels. The CL intensity was enhanced via synergistic

✉ Cheng Zhi Huang
chengzhi@swu.edu.cn

✉ Yuan Fang Li
liyf@swu.edu.cn

1 Key Laboratory of Luminescence Analysis and Molecular Sensing (Southwest University), Ministry of Education, College of Chemistry and Chemical Engineering, Southwest University, Chongqing 400715, People's Republic of China

2 Key Laboratory of Luminescent and Real-Time Analytical System (Southwest University), Chongqing Science and Technology Bureau, College of Pharmaceutical Sciences, Southwest University, Chongqing 400715, People's Republic of China

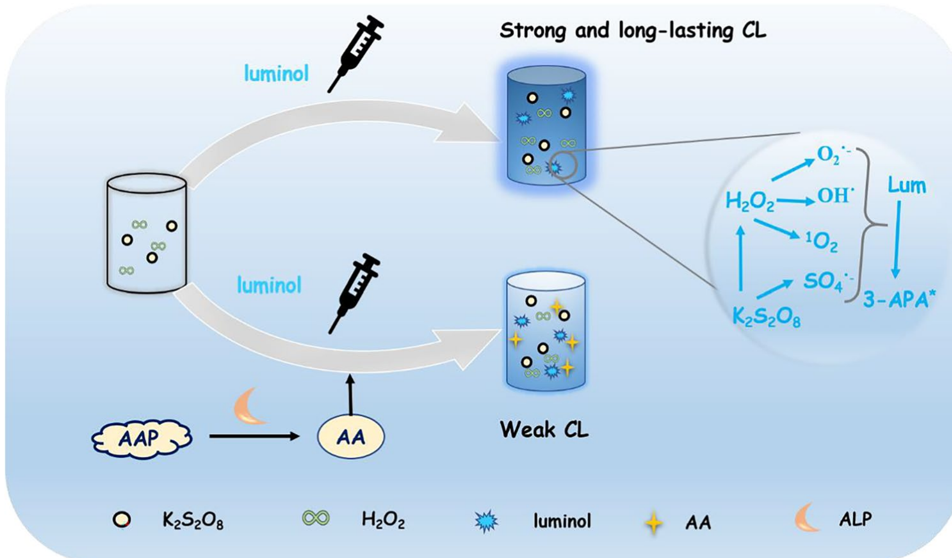

Scheme 1 Schematic demonstration of the CL behavior and the ALP detection of luminol-H_2O_2–$K_2S_2O_8$ system

catalysis of MOF-Pt and Co^{2+} [10]. Moreover, catalysts such as Cu-MOF and g-CN_{OX} nanosheets were used to catalyze H_2O_2 to continuously produce $OH^•$, $O_2^{•-}$, and $^1O_2$. The $OH^·$ and $O_2^{•-}$ were then recombined into $^1O_2$ to prolong the CL duration time of the luminol-H_2O_2 system [11, 12]. All of these CL systems realized long-lasting CL emission via the slow diffusion of hydrogels or extra catalysts, which in turn requires a complicated preparation process. Therefore, developing a simple long-lasting and catalyst-free CL reaction process is particularly critical.

The luminol-H_2O_2 system is a typical CL system. Lind et al. demonstrated that the decomposition reaction of peroxide adduct in the luminol-H_2O_2 CL system is a rate-determining kinetic step in the production of excited state [13]. Roberts group studied the reaction kinetics of luminol-H_2O_2 CL system in the presence of $K_2S_2O_8$. They found that the reaction was first order with respect to luminol and persulfate, zero order to hydrogen peroxide and base [14]. By using ammonium persulfate to enhance the intensity of luminol-H_2O_2 CL system, Dai et al. developed a CL imaging method for the rapid detection of haptoglobin phenotyping [15]. However, none of these studies investigated the long-life CL of luminol-H_2O_2 system. Here, the long-lasting mechanism of the luminol-H_2O_2–$K_2S_2O_8$ system was investigated (Scheme 1). In this CL system, H_2O_2 and $K_2S_2O_8$ co-reactants can continuously produce such radicals as $OH^•$, $^1O_2$, $O_2^{•-}$, $SO_4^{•-}$ to oxidize the luminol, which leads to intense and long-lasting emission. In addition, $K_2S_2O_8$ can react with H_2O to generate H_2O_2, which can extend the CL duration time. As a reactive hydrolase, alkaline phosphatase (ALP) is widely distributed in human tissues and body fluids and can dephosphorylate various proteins and non-proteins. Levels of ALP in human serum are vital indicator of several diseases. The normal range of serum ALP in healthy adults is 40–150 $U·L^{-1}$. Abnormal ALP concentrations can induce many diseases, including bone disease, breast cancer, diabetes, and prostate cancer [16]. Therefore, the determination of ALP in serum is critically important because it can influence treatment and recovery. Fluorescence, electrogenerated chemiluminescence, colorimetry, and surface-enhanced Raman scattering have all been proposed for ALP detection [17]. Most previous methods have suffered from a complex synthesis, and thus, it is highly desirable to develop a simple and convenient method for ALP detection. L-ascorbic acid 2-phosphate trisodium salt (AAP) can be hydrolyzed by ALP, resulting in the production of ascorbic acid (AA),[18] that can restrain reactive oxygen species (ROS) and quench the CL signal of a luminol-H_2O_2–$K_2S_2O_8$ system. In turn, a method for sensitive and selective detection of ALP was established (Scheme 1).

Experimental

Reagents and apparatus

The reagents and apparatus are descripted in the supplementary information.

Chemiluminescence measurements

All of the CL signals were measured via a BPCL luminescence analyzer, and the PMT was operated at – 900 V. In a typical CL measurement, 50 μL of 0.8 $mmol·L^{-1}$ $K_2S_2O_8$, 50 μL of 0.8 $mmol·L^{-1}$ H_2O_2, 50 μL of pH 10 BR buffer solution, and 100 μL of H_2O were added into a quartz cuvette. Next, 250 μL of 1.0 $mmol·L^{-1}$ luminol solution was rapidly injected through the static injection method to generate CL emission.

Detection of alkaline phosphatase

To achieve ALP detection, 100 μL of pH 8.5 BR buffer, 100 μL of 3 mmol·L^{-1}AAP, and 700 μL H_2O were mixed and then added to 100 μL of different concentrations of ALP. The resulting solution was then incubated at 37 ℃ with 300 r·min^{-1} for 0.5 h. Finally, 50 μL of pH 10 BR buffer, 50 μL of 0.8 mmol·L^{-1} H_2O_2, 50 μL of 0.8 mmol·L^{-1} $K_2S_2O_8$, and 50 μL of the incubated solutions were mixed. Upon 250 μL of luminol (1.0 mmol·L^{-1}) was injected into the quartz cuvette, the CL signal was collected via a BPCL analyzer.

Detection of alkaline phosphatase in human serum samples

Three samples of human blood were obtained from volunteers in accordance with the institutional committee of Southwest University. All three samples were only employed in this work. All of the experimental steps were performed in accordance with the relevant laws and the institutional regulations of ethical standards of the institutional committee of Southwest University (approval number: yxy202114).

Blood samples from volunteers were first collected in 5 mL glass tubes and allowed to clot at room temperature for 2 h, and the clotted samples were then centrifuged for 10 min at 3000 r/min^{-1}. Next, the mixture containing 50 μL 3 mmol·L^{-1} AAP, 50 μL human serum sample, 50 μL pH 8.5 BR buffer, and 350 μL H_2O were incubated at 37 ℃ and 300 r/min^{-1} for 0.5 h. Then, 50 μL of 0.8 mmol·L^{-1} $K_2S_2O_8$ and H_2O_2, 50 μL of pH 10 BR buffer solution, 50 μL the above mixed solution, and 50 μL of H_2O were added into the quartz cuvette. Finally, 250 μL of 1.0 mmol·L^{-1} luminol solution was promptly injected into the cuvette via a static injection method to initiate CL. Each sample was detected in parallel three times, and human serum samples were obtained from healthy volunteers.

Results and discussion

Chemiluminescence performance of luminol-H_2O_2–$K_2S_2O_8$ system

All the CL experiments were measured through static injection to evaluate the CL property of luminol-H_2O_2–$K_2S_2O_8$ system. Increased CL intensity in the luminol-H_2O_2–$K_2S_2O_8$ system was observed (red curve), which was 1745 and 30 times to the signal of luminol-H_2O_2 system (green curve) and luminol-$K_2S_2O_8$ system (black curve), respectively (Fig. 1A). In addition, the CL signal of luminol-H_2O_2–$K_2S_2O_8$ system decays to half after approximately

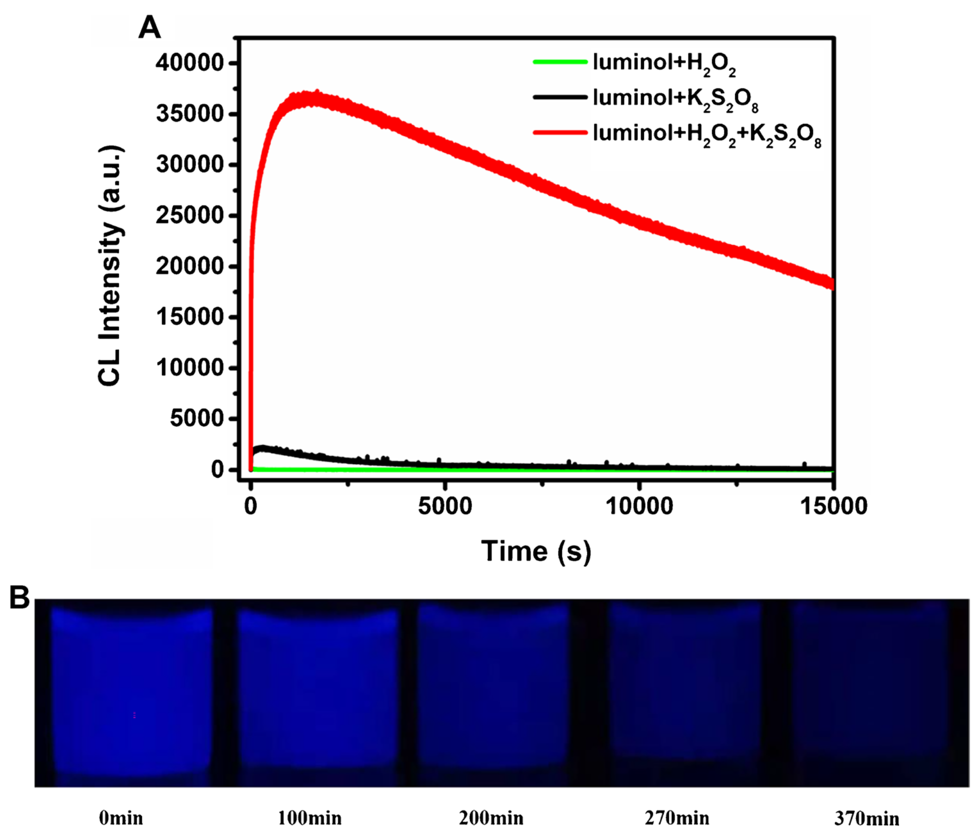

Fig. 1 **A** CL kinetic curves of luminol-H_2O_2–$K_2S_2O_8$ (red curve), luminol-H_2O_2 (green curve), and luminol-$K_2S_2O_8$ (black curve). Reaction conditions: 1.0 mmol·L^{-1} luminol, 0.8 mmol·L^{-1} H_2O_2, 0.8 mmol·L^{-1} $K_2S_2O_8$, and pH 10 BR buffer. **B** The digital photographs of luminol-H_2O_2–$K_2S_2O_8$ CL system from 0 to 370 min. Reaction conditions: 5.0 mmol·L^{-1} luminol, 4.0 mmol·L^{-1} H_2O_2, 4.0 mmol·L^{-1} $K_2S_2O_8$, and pH 10 BR buffer

4 h (Fig. 1A), thus proving the excellent CL behavior of the luminol-H_2O_2–$K_2S_2O_8$ CL system. The concentrations of luminol, H_2O_2, and $K_2S_2O_8$ were increased for visual observation of persistent CL. Blue light was observed through naked eyes in the dark for 370 min (Fig. 1B).

The intensity and duration of CL systems are associated with pH, as well as H_2O_2, $K_2S_2O_8$, and luminol concentrations. Hence, the influences of pH values and H_2O_2, $K_2S_2O_8$, and luminol concentrations for the luminol-H_2O_2–$K_2S_2O_8$ system were investigated (Fig. S1A, B, C, and D). The optimal pH value was 10. The appropriate concentration of H_2O_2 was 0.8 mmol·L^{-1}. Considering the stability of the proposed CL method for ALP detection, the optimal concentrations of $K_2S_2O_8$ and luminol were 0.8 and 1 mmol·L^{-1}, respectively. In addition, the CL intensity remained stable within 1 min (Fig. S2) and all of the CL signals were collected at 275 s in this work.

Chemiluminescence mechanism of luminol-H_2O_2–$K_2S_2O_8$ system

This long-lasting CL system was mainly composed of H_2O_2, $K_2S_2O_8$, and luminol; to adequately study the persistent CL mechanism, the CL spectra of the proposed system was thus measured. The maximum emission wavelength was ~ 425 nm, which indicated that the luminophores in this luminol-H_2O_2–$K_2S_2O_8$ system were the excited 3-aminophthalate anions (3-APA*) (Fig. 2A), consistent with previous reports [19]. The CL reactions containing H_2O_2 usually involve redox reactions of ROS such as $OH^\bullet$, $^1O_2$, and $O_2^{\bullet-}$[20]. In this system, possible sources of the ROS were associated with dissolved oxygen and H_2O_2. First, to investigate the influence of dissolved oxygen, the CL intensity of luminol-H_2O_2–$K_2S_2O_8$ systems in air-saturated, O_2-saturated, and N_2-saturated conditions were measured. Obviously, visible distinctions were observed among these three conditions. The highest CL emission was observed in O_2-saturated CL system, and the weakest CL signal appeared in N_2-saturated CL system (Fig. 2B). The experimental phenomena illustrated that the CL intensity was enhanced and accompanied by an increase in dissolved oxygen content, thus indicating that dissolved oxygen was one of the sources of ROS.

A cyclic voltammogram (CV) was also applied to further study the radical generation in luminol-H_2O_2–$K_2S_2O_8$ system (Fig. 2C). The CV reduction peak in the $K_2S_2O_8$ solution in BR was at − 1.4 V, which indicated that $S_2O_8^{2-}$ can be reduced to generate sulfate radical anion ($SO_4^{\bullet-}$) [21]. The reduction and oxidation peaks of H_2O_2 solution were at − 0.8 and 1.6 V, respectively. Only one reduction peak was observed at − 0.7 V upon mixing H_2O_2 and $K_2S_2O_8$, and this might belong to the reduction of H_2O_2. The oxidation peak of H_2O_2 was then shifted from 1.6 to 1.2 V; these results indicated that the addition of $K_2S_2O_8$ improved the production of ROS [22]. The reduction peak of $K_2S_2O_8$ also disappeared, which suggested that $S_2O_8^{2-}$ could be easily reduced into $SO_4^{\bullet-}$ upon addition of H_2O_2 [23]. Therefore, H_2O_2 and $K_2S_2O_8$ act as co-reactants in this CL system; they can work cooperatively to generate ROS and $SO_4^{\bullet-}$, respectively. Thus, a catalyst-free CL co-reaction system was developed.

The presence of $OH^\bullet$, $^1O_2$, and $O_2^{\bullet-}$ was verified via the radical inhibition experiments. The quenching efficiency was significantly enhanced with increased concentration of AA, a common radical scavenger (Fig. S3A). This result confirmed the production of ROS in this CL system. The inhibition ratio notably increased upon addition of thiourea, which is an efficient scavenger of $OH^\bullet$; this result indicated the containment of $OH^\bullet$ in this system (Fig. S3B). The CL intensity of the luminol-H_2O_2–$K_2S_2O_8$ system was also obviously decreased upon addition of tryptophan, one of scavengers of $^1O_2$,[24] thus, revealing the involvement of $^1O_2$ in the reaction (Fig. S3C). Similarly, the CL emission

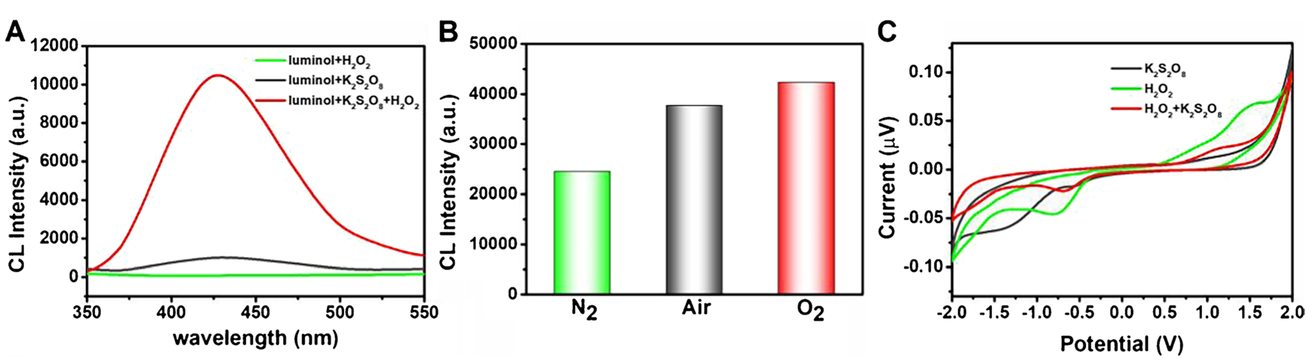

Fig. 2 **A** The CL spectra of the system: luminol-H_2O_2 (green curve), luminol-$K_2S_2O_8$ (black curve), and luminol-H_2O_2–$K_2S_2O_8$ (red curve). **B** The CL intensity at 275 s of CL reactions of luminol-H_2O_2–$K_2S_2O_8$ system under N_2-saturation solution (green column), air-saturation solution (black column), and O_2 saturation (red column). **C** The CV curves of the H_2O_2 alone (green curve), $K_2S_2O_8$ alone (black curve), and mixture of H_2O_2 and $K_2S_2O_8$. Reaction conditions: 1.0 mmol·L^{-1} luminol, 0.8 mmol·L^{-1} H_2O_2, 0.8 mmol·L^{-1} $K_2S_2O_8$, and pH 10 BR buffer

of this system was effectively inhibited in the presence of benzoquinone, demonstrating that $O_2^{\bullet-}$ was also involved in the CL reaction (Fig. S3D). Hence, ROS were proven to be crucial intermediates in this co-reaction system.

Electron spin resonance (ESR) experiments were measured to further confirm the generation of ROS and $SO_4^{\bullet-}$. Due to the respective characteristic signals, 5,5-dimethyll-pyrroline-N-oxide (DMPO) was used to capture $OH^{\bullet}$ and $SO_4^{\bullet-}$ during the CL reaction process [25]. The DMPO-$OH^{\bullet}$ and DMPO-$SO_4^{\bullet-}$ adducts were easily detected in the luminol-H_2O_2–$K_2S_2O_8$ CL system (Fig. 3A and B), thus, confirming that $OH^{\bullet}$ and $SO_4^{\bullet-}$ were generated in the CL co-reaction system. 2,2,6,6-tetramethyl-4-piperidine (TEMP) is a common scavenger of $^1O_2$ and can react with $^1O_2$ to generate 2,2,6,6-tetramethyl-4-piperidine-N-oxide (TEMPO) adduct product [26]. A typical 1:1:1 triplet signal of TEMPO was observed, thus indicating the production of $^1O_2$ (Fig. 3C and D). In addition, as shown in Fig. 3E and F, the 1:1:1:1 quartette signal of DMPO-$O_2^{\bullet-}$ also demonstrated the presence of $O_2^{\bullet-}$. Moreover, distinctly higher ESR signals were seen for $OH^{\bullet}$, $^1O_2$, $O_2^{\bullet-}$, and $SO_4^{\bullet-}$ in luminol-H_2O_2–$K_2S_2O_8$ system (Fig. 3, lines of a) than the luminol-H_2O_2 (Fig. 3, lines of c) and luminol-$K_2S_2O_8$ (Fig. 3, lines of b) systems, which further demonstrated that the coexistence of H_2O_2 and $K_2S_2O_8$ can promote each other to generate corresponding radicals. To prove the properties of the long-life CL behavior in the luminol-H_2O_2–$K_2S_2O_8$ system, the ESR spectra at different reaction intervals were measured to demonstrate the continuous generation of ROS and $SO_4^{\bullet-}$. Obviously, the CL intensities of the ESR signal from DMPO-$OH^{\bullet}$, DMPO-$SO_4^{\bullet-}$, TEMPO-$^1O_2$, as well as DMPO-$O_2^{\bullet-}$ in

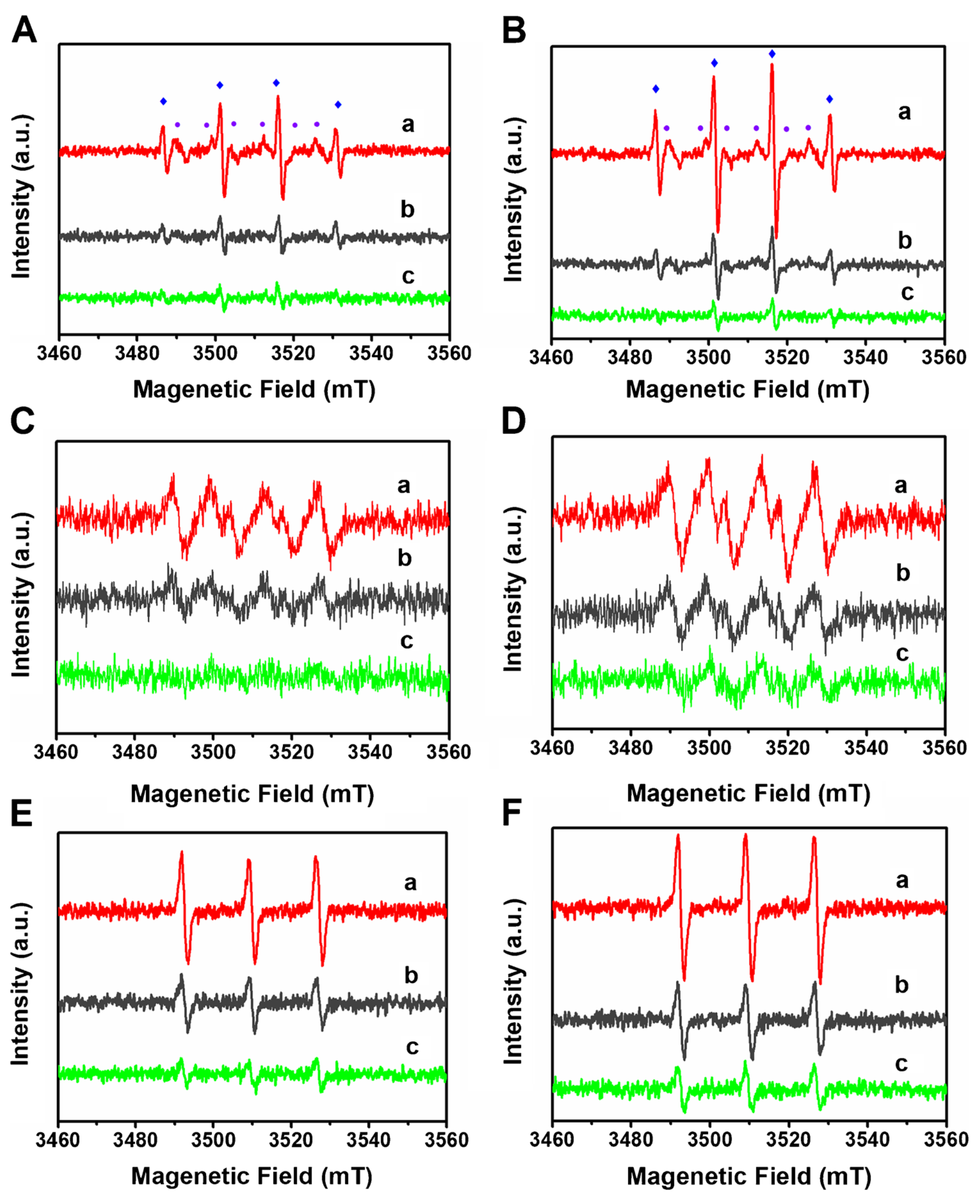

Fig. 3 ESR spectra of luminol-H_2O_2–$K_2S_2O_8$ (a. red curves), luminol-$K_2S_2O_8$ (b. black curves) system, and luminol-H_2O_2 (c. green curves). The ESR spectra of DMPO-$SO_4^{\bullet-}$(purple circle) and DMPO-$OH^{\bullet}$ (blue rhombus) adducts at 5 min (**A**) and 10 min (**B**) during the reaction, respectively. The ESR spectra of TEMPO-$^1O_2$ adducts at 5 min (**C**) and 10 min (**D**) during the reaction. The ESR spectra of DMPO-$O_2^{\bullet-}$adducts at 5 min (**E**) and 10 min (**F**) during the reaction, respectively. Reaction conditions: 1.0 mmol·L^{-1} luminol, 0.8 mmol L^{-1} H_2O_2, 0.8 mmol·L^{-1} $K_2S_2O_8$, and pH 10 BR buffer

the luminol-H_2O_2–$K_2S_2O_8$ system were obviously enhanced with the reaction progress, thus leading to glow-type CL.

According to previous reports, H_2O_2 was produced when $K_2S_2O_8$ reacted with H_2O ($K_2S_2O_8 + 2H_2O \rightarrow H_2O_2 + 2KHSO_4$) [27, 28]. Hence, we speculated that H_2O_2 was generated through the reaction between $K_2S_2O_8$ and H_2O that prolongs the CL duration time in this co-reaction system. We used 10-acetyl-3,7-dihydroxyphenoxazine (ADHP) as an excellent reagent for H_2O_2 detection, as reported previously [29]. Here, ADHP reacts with H_2O_2 to generate a red fluorescent oxidation product, resorufin, with an emission maximum of ~ 585 nm [30]. Figure 4A shows that the fluorescence spectra of resorufin are located at ~ 585 nm upon oxidation of ADHP in the presence of $K_2S_2O_8$, thus, confirming the generation of H_2O_2. In addition, luminol was dissolved in NaOH solution in our work. It was found that alkaline medium was essential to the reaction of $K_2S_2O_8$ and H_2O for the generation of H_2O_2 (Fig. S4).

Catalase was also added into the luminol-$K_2S_2O_8$ system and leads a decrease in CL signal (Fig. 4B), which further revealed the production of H_2O_2. $K_2S_2O_8$ was also added into luminol-H_2O_2–$K_2S_2O_8$ system after 340 min of CL reaction, and then the dimmed light of the CL system became brighter, thus, indicating that H_2O_2 was generated in this system (Fig. S5). These results confirm the continuous production of H_2O_2 in this co-reaction CL system, and the CL duration time was thus prolonged. Finally, the reaction rate constants (k) of luminol-H_2O_2, luminol-$K_2S_2O_8$, and luminol-H_2O_2–$K_2S_2O_8$ systems were calculated [31] to be 1.17, 0.75, and 0.19 h^{-1}, respectively (Fig. S6). The k values proved that the slow reaction rate of the co-reaction CL system indicates the long-lasting characteristic of the proposed CL system [32]. A possible mechanism for long-lasting CL in luminol-H_2O_2–$K_2S_2O_8$ system was summarized (Scheme S1) [22, 33, 34]. First, co-reactants H_2O_2 and $K_2S_2O_8$ promoted each other to produce the corresponding radicals ($SO_4^{\bullet-}$, $OH^{\bullet}$, $^1O_2$, $O_2^{\bullet-}$), thus, oxidizing luminol to 3-APA* and producing CL emission. $K_2S_2O_8$ could then react with H_2O to continuously generate the H_2O_2 during the CL reaction process, further prolonging CL duration time. Thus, a catalyst-free co-reaction CL system with an intensive and long-lasting emission was developed.

Detection of alkaline phosphatase

It is well known that AA is a common radical scavenger that can be generated through a reaction between ALP and AAP. Thus, a co-reaction CL system can be employed to detect ALP. Under optimum experimental conditions (Fig. S7), changes in CL intensity (ΔI) were enhanced with increasing ALP concentration (Fig. 5A). The ΔI was linear with the logarithm of ALP concentration from 0.08 to 5 $U{\cdot}L^{-1}$ as given by $\Delta I = 13{,}883.3 \lg c_{ALP} - 22{,}110.1$, $R^2 = 0.992$, and the limit of detection (LOD) of ALP is 0.049 U/L (inset of Fig. 5A). Herein, c_{ALP} represents the ALP concentration, and I_0, I_s represent the CL intensity in the absence (I_0) and presence (I_s) of ALP, respectively.

The influence of potential interfering substance was investigated to evaluate the specificity of the proposed approach for the ALP detection. We compared the ΔI in the coexistence of ALP and some common interfering amino acids or ions in the serum samples. The addition of these interference factors negligibly influenced ΔI (Fig. 5B). These results indicated that the method of ALP detection reported here is not affected by the interference substances in human serum. To further investigate the selectivity of this method for ALP, several interfering proteins and enzymes, including bovine serum albumin (BSA, b), glucose oxidase (GO, c), human serum albumin (HAS, d), lysozyme (e), trypsin (f), and acetylcholinesterase (AChE, g), were investigated

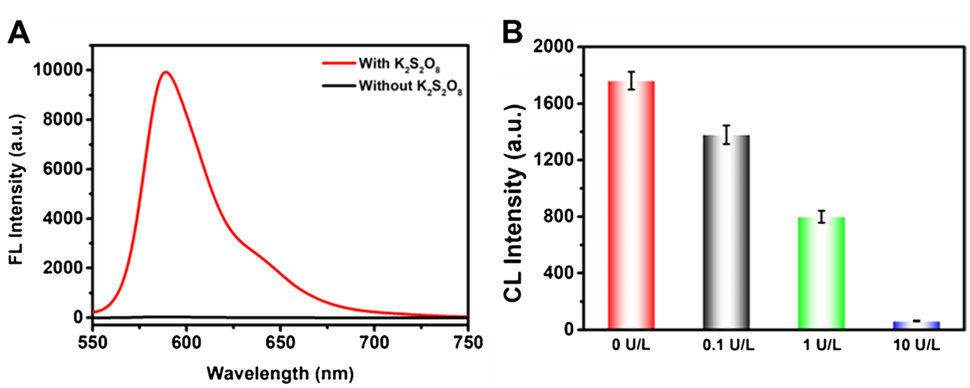

Fig. 4 **A** The fluorescence spectra of ADHP at the present (red line) and absent (black line) of $K_2S_2O_8$ solution. Reaction conditions: 0.8 $mmol{\cdot}L^{-1}$ $K_2S_2O_8$, 2 $mmol{\cdot}L^{-1}$ NaOH, pH 10 BR buffer, and 0.2 $mmol{\cdot}L^{-1}$ ADHP. **B** The CL intensity at 275 s of the luminol-$K_2S_2O_8$ system under different catalase concentrations. Reaction conditions: 1.0 $mmol{\cdot}L^{-1}$ luminol, 0.8 $mmol{\cdot}L^{-1}$ H_2O_2, 0.8 $mmol{\cdot}L^{-1}$ $K_2S_2O_8$, and pH 10 BR buffer. The concentrations of catalase were 0 $U{\cdot}L^{-1}$ (red column), 0.1 $U{\cdot}L^{-1}$ (black column), 1 $U{\cdot}L^{-1}$ (green column), 10 $U{\cdot}L^{-1}$ (blue column)

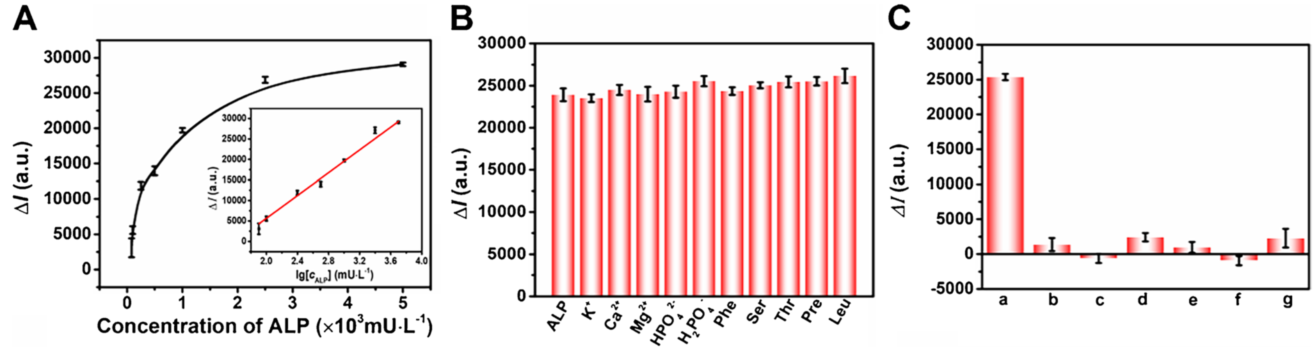

Fig. 5 ALP detection in the luminol-H_2O_2–$K_2S_2O_8$ CL system. **A** Calibration curve of ALP. Inset: linear calibration plot for ALP ranged from 0.08 to 5 U·L^{-1}, $R^2=0.992$. **B** Interference study of luminol-H_2O_2–$K_2S_2O_8$ CL system. Reaction conditions: 1.0 mmol·L^{-1} luminol, 0.8 mmol·L^{-1} H_2O_2, 0.8 mmol·L^{-1} $K_2S_2O_8$, pH 10 BR buffer, 3 mmol·L^{-1} AAP, 5 mmol·L^{-1} K^+, 2.5 mmol·L^{-1} Ca^{2+}, 1 mmol·L^{-1} Mg^{2+}, 1 mmol·L^{-1} HPO_4^{2-}, 1 mmol·L^{-1} $H_2PO_4^-$, 200 μmol·L^{-1} serine, 200 μmol·L^{-1} proline, 200 μmol·L^{-1} leucine, 100 μmol·L^{-1} phenylalanine, and 100 μmol·L^{-1} threonine. **C** Selectivity study of the luminol-H_2O_2–$K_2S_2O_8$ CL system. Reaction conditions: 3 U·L^{-1} ALP, 30 U·L^{-1} GO, lysozyme, trypsin and AChE, 3 μmol·L^{-1} BSA, and HAS

under the same condition to the system (Fig. 5C). The results demonstrated that none of these proteins or enzymes has an obvious effect on the system compared with ALP, illustrating the high selectivity of this method for ALP detection. We next verified the feasibility of this approach by studying the recoveries of ALP through adding a determined amount standard solution of ALP into human serum samples. As shown in Table S1, the averaged spiked recoveries of ALP ranged from 92.0 to 106.1%, illustrating that the proposed approach could sensitively detect ALP in human serum samples. Versus previously reported methods (Table S2), this assay is simple (requires no materials) and sensitive.

Conclusions

In summary, we prepared a catalyst-free co-reaction luminol-H_2O_2–$K_2S_2O_8$ CL system, showing long-lasting and intense CL emission that can last for up to 6 h. The mechanism of the long-lasting CL emission was attributed to the concurrence of H_2O_2 and $K_2S_2O_8$ that leads to the generation of $OH^•$, $^1O_2$, $O_2^{•-}$, and $SO_4^{•-}$. Furthermore, owing to the reaction of $K_2S_2O_8$ and H_2O, the continuous production of H_2O_2 in this luminol-H_2O_2–$K_2S_2O_8$ system further enhances the CL emission lifetime. This catalyst-free co-reaction CL system was then successfully used to detect ALP. This approach offers new methods to study long-lasting CL systems and harnesses their potential in related fields.

Supplementary Information The online version contains supplementary material available at https://doi.org/10.1007/s00604-022-05287-5.

Funding This work was financially supported by the National Natural Science Foundation of China (NSFC, no. 21874109).

Declarations

Ethics approval This study was approved by the institutional committee of Southwest University (approval number: yxy202114).

Conflict of interest The authors declare no competing interests.

References

1. Li F, Guo L, Li ZM, He JB, Cui H (2020) Temporal-spatial-color multiresolved chemiluminescence imaging for multiplex immunoassays using a smartphone coupled with microfluidic chip. Anal Chem 92:6827–6831
2. Gnaim S, Scomparin A, Das S, Blau R, Satchi-Fainaro R, Shabat D (2018) Direct real-time monitoring of prodrug activation by chemiluminescence. Angew Chem In Ed 57:9033–9037. https://doi.org/10.1002/anie.201804816
3. Xiao ZY, Wang YT, Xu B, Du SF, Fan WD, Cao DW, Deng Y, Zhang LL, Wang L, Sun DF (2020) An integrated chemiluminescence microreactor for ultrastrong and long-lasting light emission. Adv Sci 7:2000065
4. Adams ST, Mofford DM, Reddy GSKK, Miller SC (2016) Firefly luciferase mutants allow substrate-selective bioluminescence imaging in the mouse brain. Angew Chem In Ed 55:4943–4946. https://doi.org/10.1002/anie.201511350
5. Xie Q, Mao GB, Chen YS, Ji XH, He ZK (2020) Long-lasting chemiluminescence hydrogels made in situ. Mater Lett 263:127205. https://doi.org/10.1016/j.matlet.2019.127205
6. Jie X, Yang H, Wang M, Zhang Y, Wei W, Xia Z (2017) A Peroxisome-inspired chemiluminescent silica nanodevice for the intracellular detection of biomarkers and its application to insulin-sensitizer screening. Angew Chem In Ed 56:14596–14601. https://doi.org/10.1002/anie.201708958
7. Li D, Zhang S, Feng X, Yang H, Nie F, Zhang W (2019) A novel peroxidase mimetic Co-MOF enhanced luminol chemiluminescence and its application in glucose sensing. Sensor Actuat B-Chem 296:126631. https://doi.org/10.1016/j.snb.2019.126631
8. Liu YT, Shen W, Li Q, Shu JN, Gao LF, Ma MM, Wang W, Cui H (2017) Firefly-mimicking intensive and long-lasting

chemiluminescence hydrogels. Nat Commun 8:1003. https://doi.org/10.1038/s41467-017-01101-6
9. Wu H, Zhao M, Li J, Zhou X, Yang T, Zhao D, Liu P, Ju H, Cheng W, Ding S (2020) Novel protease-free long-lasting chemiluminescence system based on the Dox-ABEI chimeric magnetic DNA hydrogel for ultrasensitive immunoassay, Acs Appl. Mater Inter 12:47270–47277. https://doi.org/10.1021/acsami.0c14188
10. Ye L, Min W, Chenchen W, Wei W, Yong L (2020) Enhancing hydrogel-based long-lasting chemiluminescence by a platinum-metal organic framework and its application in array detection of pesticides and d-amino acids. Nanoscale 12:4959–4967. https://doi.org/10.1039/D0NR00203H
11. Sun XQ, Lei J, Jin Y, Li BX (2020) Long-lasting and intense chemiluminescence of luminol triggered by oxidized g-C_3N_4 nanosheets. Anal Chem 92:11860–11868. https://doi.org/10.1021/acs.analchem.0c02221
12. Yang CP, He L, Huang CZ, Li YF, Zhen SJ (2021) Continuous singlet oxygen generation for persistent chemiluminescence in Cu-MOFs-based catalytic system. Talanta 221:121498. https://doi.org/10.1016/j.talanta.2020.121498
13. Merenyi G, Lind JS (1980) Role of a peroxide intermediate in the chemiluminescence of luminol. Mechanistic Study, J Am Chem Soc 102:5830–5835. https://doi.org/10.1021/ja00538a022
14. Rauhut MM, Semsel AM, Roberts BG (1966) Reaction rates, quantum yields, and partial mechanism for the chemiluminescent reaction of 3-Aminophthalhydrazide with aqueous alkaline hydrogen peroxide and persulfate1. J Org Chem 31:2431–2436. https://doi.org/10.1021/jo01346a001
15. Huang G, Ouyang J, Delanghe JR, Baeyens WRG, Dai Z (2004) Chemiluminescent image detection of haptoglobin phenotyping after polyacrylamide gel electrophoresis. Anal Chem 76:2997–3004. https://doi.org/10.1021/ac035109e
16. Zeng Y, Ren J-Q, Wang S-K, Mai J-M, Qu B, Zhang Y, Shen A-G, Hu J-M (2017) Rapid and reliable detection of alkaline phosphatase by a hot spots amplification strategy based on well-controlled assembly on single nanoparticle. Acs Appl Mater Inter 9:29547–29553. https://doi.org/10.1021/acsami.7b09336
17. Han Y, Chen J, Li Z, Chen H, Qiu H (2020) Recent progress and prospects of alkaline phosphatase biosensor based on fluorescence strategy. Biosens Bioelectron 148:111811. https://doi.org/10.1016/j.bios.2019.111811
18. He Y, Jiao BN (2017) Determination of the activity of alkaline phosphatase based on the use of ssDNA-templated fluorescent silver nanoclusters and on enzyme-triggered silver reduction, Microchim. Acta 184:4167–4173. https://doi.org/10.1007/s00604-017-2459-x
19. Wang DM, Gao MX, Gao PF, Yang H, Huang CZ (2013) Carbon nanodots-catalyzed chemiluminescence of luminol: a singlet oxygen-induced mechanism. J Phys Chem C 117:19219–19225. https://doi.org/10.1021/jp404973b
20. He L, Peng ZW, Jiang ZW, Tang XQ, Huang CZ, Li YF (2017) Novel iron(III)-based metal-organic gels with superior catalytic performance toward luminol chemiluminescence, Acs Appl. Mater Inter 9:31834–31840. https://doi.org/10.1021/acsami.7b08476
21. Xiao SY, Li Y, Zhen SJ, Huang CZ, Li YF (2020) Efficient peroxydisulfate electrochemiluminescence system based the novel silver metal-organic gel as an effective enhancer. Electrochim Acta 357:136842. https://doi.org/10.1016/j.electacta.2020.136842
22. Zhang QR, Dai H, Wang T, Li YL, Zhang SP, Xu GF, Chen SH, Lin YY (2016) Ratiometric electrochemiluminescent immunoassay for tumor marker regulated by mesocrystals and biomimetic catalyst. Electrochim Acta 196:565–571. https://doi.org/10.1016/j.electacta.2016.02.202
23. Li CY, Gao JH, Yi J, Zhang XG, Cao XD, Meng M, Wang C, Huang YP, Zhang SJ, Wu DY, Wu CL, Xu JH, Tian ZQ, Li JF (2018) Plasmon-Enhanced Ultrasensitive Surface Analysis Using Ag Nanoantenna. Anal Chem 90:2018–2022. https://doi.org/10.1021/acs.analchem.7b04113
24. Rasmus Lybech J, Jacob A, Peter RO (2012) Reaction of singlet oxygen with tryptophan in proteins: a pronounced effect of the local environment on the reaction rate. J Am Chem Soc 134:9820–9826. https://doi.org/10.1021/ja303710m
25. Anqi W, Hui W, Hao D, Shu W, Wei S, Zixiao Y, Rongliang Q, Kai Y (2019) Controllable synthesis of mesoporous manganese oxide microsphere efficient for photo-Fenton-like removal of fluoroquinolone antibiotics. Appl Catal B-Environ 238:298–308. https://doi.org/10.1016/j.apcatb.2019.02.034
26 Na Y, Hongjie S, Xiangyu W, Xiaoqing F, Yingying S, Yi L (2015) A metal (Co)–organic framework-based chemiluminescence system for selective detection of l-cysteine. Analyst 140:2656–2663. https://doi.org/10.1039/C5AN00022J
27. Bornemann K (1903) Beiträge zur Kenntnis des Wasserstoffsuperoxyds. Z Anorg Chem 34:1–42. https://doi.org/10.1002/zaac.19030340102
28. Solanki DN, Kamath ISK (1946) The electrolytic preparation of hydrogen peroxide. Proc Indian Acad Sci - Section A 24:305–314. https://doi.org/10.1007/BF03171065
29. Mohanty JG, Jaffe JS, Schulman ES, Raible DG (1997) A highly sensitive fluorescent micro-assay of H_2O_2 release from activated human leukocytes using a dihydroxyphenoxazine derivative. J Immunol Methods 202:133–141. https://doi.org/10.1016/S0022-1759(96)00244-X
30. Kim S-H, Kim B, Yadavalli VK, Pishko MV (2005) Encapsulation of enzymes within polymer spheres to create optical nanosensors for oxidative stress. Anal Chem 77:6828–6833. https://doi.org/10.1021/ac0507340
31. Wu Y, Li X, Yang Q, Wang D, Yao F, Cao J, Chen Z, Huang X, Yang Y, Li X (2020) Mxene-modulated dual-heterojunction generation on a metal-organic framework (MOF) via surface constitution reconstruction for enhanced photocatalytic activity. Chem Eng J 390:124519. https://doi.org/10.1016/j.cej.2020.124519
32. Yang Z, Xia X, Shao L, Wang L, Liu Y (2021) Efficient photocatalytic degradation of tetracycline under visible light by Z-scheme Ag_3PO_4/mixed-valence MIL-88A(Fe) heterojunctions: Mechanism insight, degradation pathways and DFT calculation. Chem Eng J 410:128454. https://doi.org/10.1016/j.cej.2021.128454
33. He L, Jiang ZW, Li W, Li CM, Huang CZ, Li YF (2018) In situ synthesis of gold nanoparticles/metal-organic gels hybrids with excellent peroxidase-like activity for sensitive chemiluminescence detection of organophosphorus pesticides. Acs Appl Mater Inter 10:28868–28876. https://doi.org/10.1021/acsami.8b08768
34. Yao W, Wang L, Wang H, Zhang X (2008) Cathodic electrochemiluminescence behavior of norfloxacin/peroxydisulfate system in purely aqueous solution. Electrochim Acta 54:733–737. https://doi.org/10.1016/j.electacta.2008.06.067

Publisher's note Springer Nature remains neutral with regard to jurisdictional claims in published maps and institutional affiliations.